KYBERNETIKA — VOLUME *53* (2017), NUMBER 4, PAGES 653–678

DISTURBANCE OBSERVER-BASED SECOND ORDER SLIDING MODE ATTITUDE TRACKING CONTROL FOR FLEXIBLE SPACECRAFT

Chutiphon Pukdeboon and Anuchit Jitpattanakul

This paper presents a composite controller that combines nonlinear disturbance observer and second order sliding mode controller for attitude tracking of flexible spacecraft. First, a new nonsingular sliding surface is introduced. Then, a second order sliding mode attitude controller is designed to achieve high-precision tracking performance. An extended state observer is also developed to estimate the total disturbance torque consisting of environmental disturbances, system uncertainties and flexible vibrations. The estimated result is used as feed-forward compensation. Although unknown bounded disturbances, inertia uncertainties and the coupling effect of flexible modes are taken into account, the resulting control method offers robustness and finite time convergence of attitude maneuver errors. Finite-time stability for the closed-loop system is rigorously proved using the Lyapunov stability theory. Simulation results are presented to demonstrate the effectiveness and robustness of the proposed control scheme.

Keywords: second order sliding mode control, flexible spacecraft, extended state observer, finite-time convergence

Classification: 93C10, 93C95, 93D15

1. INTRODUCTION

With the development of space technology, modern spacecraft missions are expected to achieve fast slewing and high-precision attitude control of spacecraft, such as navigation, communication and earth observations. In practical applications, the attitude of flexible spacecraft are inevitably affected by space environmental disturbances, vibrations of flexible appendages, inertia uncertainties caused by fuel consumptions and load variations. These factors may reduce pointing accuracy of the attitude of flexible spacecraft and even cause instability. Thus, it is very challenging to design an attitude controller for flexible spacecraft to achieve rapid and precise maneuver performance. Various control methods have been applied to deal with this problem, such as passivity-based control [6, 9], sliding mode control (SMC) [1, 11, 13], active disturbance rejection control [3, 4], backstepping control [14] and so forth [7, 19, 31]. Although these methods have provided for sufficient reliable results, they can only ensure the asymptotic convergence. In other words, the attitude converges to the desired attitude with infinite settling time.

DOI: 10.14736/kyb-2017-4-0653

However, in some scenarios, infinite time attitude control is inadequate and the ability of fast maneuver is required in many real-time space missions. To obtain rapid convergence speed and enhance system robustness, finite-time control strategies are usually required [8, 34]. Finite-time stability [2, 22] implies finite-time convergence of system trajectories. It achieves faster convergence and better disturbance rejection than asymptotic or exponential stability. Terminal sliding mode control (TSMC) has offered a practical way to obtain convergence of system state in finite time [20, 31]. TSMC has been applied in [12, 27] to deal with spacecraft attitude control problems. However, the traditional TSMC methods encountered singularity problem. Later, to solve the singularity problem, nonsingular terminal sliding mode control techniques [10, 33] which are the enhanced TSMC methods have been developed. Nonsingular terminal sliding mode control techniques have been used to design attitude control laws in [18, 24, 30]. Recently second order sliding mode control (SOSMC) [15] is considered as a potential method to alleviate the control chattering and offer higher tracking accuracy when compared to the conventional SMC. Pukdeboon et al. [23], [25] developed SOSMC algorithms for spacecraft attitude tracking maneuvers. Shtessel et al. [26] applied a smooth SOSMC law to a missile guidance system. Tiwari et al. [28] used the geometric homogeneity approach to design a globally robust SOSMC scheme for attitude tracking of a rigid spacecraft. Li et al. [17] proposed an SOSMC algorithm for spacecraft formation flying. Davila et al. [15] applied a second order sliding mode observer to mechanical systems.

Extended state observer (ESO) has been considered as an effective approach to compensate for uncertainties and disturbances. Several researches have incorporated ESO into SMC method to obtain strong robustness. In Xia et al. [32] attitude tracking control scheme was developed using SMC and ESO was applied to estimate bounded disturbance. In [16] the ESO technique and the control Lyapunov function approach are merged to design an attitude controller under actuator saturation. Zhong et al. [35] developed a robust ESO-based SMC scheme to control attitude tracking and vibration suppression of flexible spacecraft. These ESO-based SMC schemes provide better robustness than the common SMC. Thus, a control technique combining ESO and SOSMC can ensure outstanding control performance for flexible spacecraft attitude maneuver.

In this paper, a new ESO and SOSMC algorithm are developed to deal with the attitude tracking problem of a flexible spacecraft in the presence of bounded disturbance and inertia uncertainties. The proposed composite attitude controller is designed combing the derived SOSMC and ESO to achieve rapid convergence, high-precision tracking performance, reduction of the vibration. The main contribution of this paper is twofold.

(1) The integrated controller combining ESO and SOSMC has rarely been studied to design a controller of complicated systems. To the best our knowledge, a combined attitude controller incorporating ESO and SOSMC has not been developed to deal with the problem of flexible spacecraft attitude tracking maneuver.

(2) A new modified nonsingular terminal sliding surface is suggested. Then, a new SOSMC attitude control algorithm with this sliding surface is designed. A novel ESO is also developed to estimate the disturbance torque and the estimated results are used as feedforward compensation. The proposed controller and disturbance observer designs are the generalized versions of the super twisting algorithm [15] and the observer presented by [5]. The proposed method gives an additional appealing feature that it offers

more choices to tune the control and observer to achieve an improved performance. The associated stability proof is accomplished by a novel strict Lyapunov function and Lyapunov stability theory.

The organization of the paper is as follows: Section 2 describes spacecraft attitude dynamics and mathematical preliminaries. Section 3 provides the chattering-free attitude controller design procedure. In section 4, the proposed ESO is presented. The finite-time convergence of of the state observer is ensured. Simulations are provided in section 5, and finally conclusion is given in section 6.

2. NONLINEAR MODEL OF SPACECRAFT AND PROBLEM FORMULATION

2.1. Spacecraft attitude dynamics and kinematics

The flexible spacecraft consists of a main rigid body and attached appendages. The reaction wheel assemblies are employed to control attitude of spacecraft. The dynamics of a spacecraft with flexible appendages can be modeled as the following nonlinear equations [6]:

$$J\dot{\omega} + \omega^{\times}\left(J\omega + \delta\dot{\eta}\right) + \delta\ddot{\eta} = u + d \tag{1}$$

$$\ddot{\eta} + C\dot{\eta} + K\eta = -\delta^{T}\dot{\omega} \tag{2}$$

where $J \in R^{3\times 3}$ is the symmetric inertia matrix of the whole structure, $\omega \in R^3$ is the angular velocity of the spacecraft in the body frame, $u \in R^3$ is the control torque acting on the hub, $d \in R^3$ is the external disturbance torque vector, and $\eta \in R^n$ is the modal coordinate vector of the flexible appendages with n being the number of flexible modes considered. In (1), $\delta \in R^{3\times n}$ is the coupling matrix between the flexible appendage and the hub, $K = \mathrm{diag}(\zeta_1^2, \cdots, \zeta_n^2)$ denotes the stiffness matrix, $C = \mathrm{diag}(2\xi_1\zeta_1, \cdots, 2\xi_n\zeta_n)$ represents the damping matrix with ζ and ξ being the natural frequency and corresponding damping. The operator $(\cdot)^{\times}$ denotes a 3×3 symmetric matrix such as

$$\omega^{\times} = \begin{bmatrix} 0 & -\omega_3 & \omega_2 \\ \omega_3 & 0 & -\omega_1 \\ -\omega_2 & \omega_1 & 0 \end{bmatrix} \tag{3}$$

for $\omega = \begin{bmatrix}\omega_1 & \omega_2 & \omega_3\end{bmatrix}^T$.

Let the vector $Q = \begin{bmatrix} q_0 & q^T \end{bmatrix}^T$ represent the attitude quaternion of the spacecraft subject to the unity length constraint, i.e $\|Q\| = 1$, where q_0 and $q = \begin{bmatrix} q_1 & q_2 & q_3\end{bmatrix}$ denote the scalar and the vector components of the unit quaternion, respectively. Attitude kinematics of spacecraft can be described by using the unit quaternion as follows [6]

$$\dot{Q} = \frac{1}{2}\begin{bmatrix} -q_v^T \\ q_0 I_3 + q^{\times}\end{bmatrix}\omega, \tag{4}$$

where I_3 is the 3×3 identity matrix.

Let $Q_d = \begin{bmatrix} q_{d0} & q_d^T\end{bmatrix}^T$ with $q_d = \begin{bmatrix} q_{d1} & q_{d2} & q_{d3}\end{bmatrix}^T$ be the unit quaternion representing the desired attitude and satisfying $\|Q_d\| = 1$. Let $\omega_r \in R^3$ be the desired angular velocity. The quaternion error $Q_e = \begin{bmatrix} q_{e0} & q_e^T \end{bmatrix}^T$ with $q_e = \begin{bmatrix} q_{1e}, q_{2e}, q_{3e} \end{bmatrix}^T$ and the angular velocity error ω_e are defined as follows:

$$q_e = q_{d0}q - q_d^{\times} q - q_0 q_d,\ q_{0e} = q^T q_d + q_0 q_{d0} \tag{5}$$

$$\omega_e = \omega - \omega_r, \tag{6}$$

The unit quaternion Q_e satisfies $\|Q_e\| = 1$. Under the coordinate given in (5) and (6), the equations (1) and (4) can be written as [6]:

$$J\dot{\omega}_e = -J\dot{\omega}_r - \omega^{\times} J\omega + u + d - \delta\ddot{\eta} - \omega^{\times}\delta\dot{\eta} \tag{7}$$

$$\dot{Q}_e = \frac{1}{2}\begin{bmatrix} -q_e^T \\ q_{e0}I_3 + q_e^{\times} \end{bmatrix}\omega_e. \tag{8}$$

We now give some lemmas that will be used in later sections.

Lemma 2.1. (Bhat and Bernstein [2]) Suppose $V(x)$ is a smooth positive definite function (defined on $U \subset R^n$) and $\dot{V}(x) + \varsigma V^{\iota}(x)$ is negative semi-definite on $U \subset R^n$ for $\iota \in (0,1)$ and $\varsigma \in R^+$, then there exists an area $U_0 \subset R^n$ such that any $V(x)$ which starts from $U_0 \subset R^n$ can reach $V(x) \equiv 0$, in finite time. Moreover, if T_r is the time needed to reach $V(x) \equiv 0$ then

$$T_r \le \frac{V^{1-\iota}(x_0)}{\varsigma(1-\iota)}, \tag{9}$$

where $V(x_0)$ is the initial value of $V(x)$.

Lemma 2.2. (Yu et al. [33]) For any numbers $\lambda_1 > 0$, $\lambda_2 > 0$, $0 < \varpi < 1$, an extended Lyapunov condition of finite-time stability can be given in the form of fast terminal sliding mode as

$$\dot{V}(x) + \lambda_1 V(x) + \lambda_2 V^{\varpi}(x) \le 0,$$

where the settling time can be estimated by

$$T_r \le \frac{1}{\lambda_1(1-\varpi)} \ln\left(\frac{\lambda_1 V^{1-\varpi}(x_0) + \lambda_2}{\lambda_2}\right). \tag{10}$$

Assumption 2.3. We assume that the inertia matrix in (7) is in the form $J = J_0 + \Delta J$ where J_0 is the known nonsingular constant matrix and ΔJ denotes the uncertainties.

Assumption 2.4. The total uncertainty vector $\tilde{d}$ and its first time derivative $\dot{\tilde{d}}$ are assumed to be bounded, but the upper bounds of $\tilde{d}$ and $\dot{\tilde{d}}$ are unknown in advance, i. e. $\|\tilde{d}\| \le D_1$, and $\|\dot{\tilde{d}}\| \le D_2$, where D_1 and D_2 are unknown positive constants.

According to Assumption 2.4, the spacecraft dynamics can be written as

$$J_0\dot{\omega}_e = -J_0\dot{\omega}_r - \omega^\times J_0\omega + u + T_d, \tag{11}$$

where

$$T_d = d - \Delta J\dot{\omega}_r - \omega^\times \Delta J\omega - \delta\ddot{\eta} - \omega^\times \delta\dot{\eta}.$$

Now, we consider the following coordinate transformation

$$\sigma = \omega_e + K_1 q_e, \tag{12}$$

where $K_1 = \mathrm{diag}(k_1, k_2, k_3)$ is a diagonal matrix with $k_i,\ i = 1, 2, 3$ being positive constants. The derivative of σ with respect to time can be obtained as

$$\begin{aligned}\dot{\sigma} &= \dot{\omega}_e + K_1\dot{q}_e \\ &= J_0^{-1}\Big(- \omega^\times J_0\omega - J_0\dot{\omega}_r + u + T_d\Big) \\ &\quad + \frac{1}{2}K_1(q_{e0}I_3 + q_e^\times)\omega_e.\end{aligned} \tag{13}$$

which can be written as

$$\dot{\sigma} = F + Bu + \tilde{d}, \tag{14}$$

where $F = J_0^{-1}\Big(- \omega^\times J_0\omega - J_0\dot{\omega}_r\Big) + \frac{1}{2}K_1(q_{e0}I_3 + q_e^\times)\omega_e$, $B = J_0^{-1}$ and $\tilde{d} = J_0^{-1}T_d$.

In this paper the disturbance $\tilde{d}$ in (14) can be rearranged as $\tilde{d} = J_0^{-1}T_d$ which satisfies the invariance condition [29]. In other words, the disturbance acts on the same channel as that of control input. Thus, the proposed control law can effectively handle matched uncertainty or disturbance.

Remark 2.5. For Assumption 2.4, it is reasonable, because the external unknown disturbances including environmental disturbance, solar radiation and magnetic effects are all bounded in in practice.

2.2. Problem Statement

In this paper, the attitude tracking control system described by (7) and (8) is considered and q_d, ω_d and $\dot{\omega}_d$ are assumed to be bounded. The main objective is to design a control law which forces the attitude and angular velocity states to a small region around the origin in finite time. This can be expressed as

$$\lim_{t\to T}(q_e(t), \omega_e(t)) \in \Omega_c \tag{15}$$

where T is a finite time and Ω_c denotes an open set around the origin.

3. FINITE-TIME SECOND ORDER SLIDING MODE ATTITUDE CONTROL

In this section, a robust finite-time attitude controller is developed to achieve rapid maneuver and high-precise attitude control performance for a flexible spacecraft in presence of external disturbances and inertia uncertainties. A new nonsingular sliding surface is constructed and then the proposed attitude controller is designed based on a new SOSMC algorithm. This controller guarantees that attitude and angular velocity errors convergence to a small neighborhood of zero in finite time. Define a sliding variable s as

$$s = \sigma + \int_0^t \Big(C_1 \Lambda_1(\sigma, \alpha)\sigma + C_2 \Lambda_2(\sigma, \gamma)\mathrm{sign}(\sigma) \Big) \mathrm{d}\tau, \tag{16}$$

where $\alpha = [\alpha_1 \quad \alpha_2 \quad \alpha_3]^T$ with $\alpha_i > 0, \quad (i = 1, 2, 3)$, $C_1 = \mathrm{diag}(c_{11}, c_{12}, c_{13})$ and $C_2 = \mathrm{diag}(c_{21}, c_{22}, c_{23})$ are diagonal matrices with c_{1i}, $c_{2i} \quad (i = 1, 2, 3)$ being positive constants. The function $\Lambda_1(\sigma, \alpha)$ is defined as

$$\Lambda_1(\sigma, \alpha) = \mathrm{diag}(\mathrm{e}^{\alpha_1|\sigma_1|}, \mathrm{e}^{\alpha_2|\sigma_2|}, \mathrm{e}^{\alpha_3|\sigma_3|}),$$

where e is the Euler number and $\alpha_i \quad (i = 1, 2, 3)$ are positive constants. In (16), for any vector $a = [a_1 \quad a_2 \quad a_3]^T$ and $0 < \gamma < 1$, we define the following functions:

$$\Lambda_2(a, \gamma) = \mathrm{diag}(|a_1|^\gamma, |a_2|^\gamma, |a_3|^\gamma) \quad \text{and} \quad \mathrm{sign}(a) = \begin{bmatrix} \mathrm{sign}(a_1) \\ \mathrm{sign}(a_2) \\ \mathrm{sign}(a_3) \end{bmatrix}.$$

During the sliding mode, the conditions $s = 0$ and $\dot{s} = 0$ are satisfied. Thus, the sliding mode dynamics can be obtained in the scalar form as

$$\dot{\sigma}_i = -c_{1i}\mathrm{e}^{\alpha_i|\sigma_i|}\sigma_i - c_{2i}|\sigma_i|^\gamma \mathrm{sign}(\sigma_i), \quad i = 1, 2, 3. \tag{17}$$

Theorem 3.1. The states $\sigma_i = 0 \quad (i = 1, 2, 3)$ of the sliding mode dynamics (17) converge to zero in finite time and the settling time is estimated by

$$T_s \leq \frac{1}{\kappa_1(1-\varpi)} \ln \left(\frac{\kappa_1 V_1^{1-\varpi}(\sigma_i(0)) + \kappa_2}{\kappa_2} \right), \tag{18}$$

where $\kappa_1 = 2c_{1i}$, $\kappa_2 = 2^{\frac{\gamma+1}{2}} c_{2i}$ and $\varpi = \frac{\gamma+1}{2}$.

Proof. The Lyapunov function candidate is chosen as

$$V_1 = \frac{1}{2}\sigma_i^2. \tag{19}$$

Its first time derivative is

$$\begin{aligned} \dot{V}_1 &= \sigma_i \dot{\sigma}_i \\ &= \sigma_i \Big(- c_{1i}\sigma_i e^{(\alpha_i|\sigma_i|)} - c_{2i}|\sigma_i|^\gamma \mathrm{sign}(\sigma_i) \Big) \\ &= -c_{1i} e^{(\alpha_i|\sigma_i|)} \sigma_i^2 - c_{2i}|\sigma_i|^{\gamma+1} \\ &= -c_{1i} e^{(\alpha_i|\sigma_i|)} V_1 - c_{2i} V_1^{\frac{\gamma+1}{2}}. \end{aligned} \tag{20}$$

For $\alpha_i > 0$, one has $e^{(\alpha_i|\sigma_i|)} > e^0 = 1$ and it follows that

$$\begin{aligned} \dot{V}_1 &\leq -2c_{1i}V_1 - 2^{\frac{\gamma+1}{2}} c_{2i} V_1^{\frac{\gamma+1}{2}} \\ &\leq \kappa_1 V_1 - \kappa_2 V_1^{\frac{\gamma+1}{2}}, \end{aligned} \tag{21}$$

where $\kappa_1 = 2c_{1i}$ and $\kappa_2 = 2^{\frac{\gamma+1}{2}}c_{1i}$. By Lemma 2.2 one can conclude that $s_i = 0$ $(i = 1, 2, 3)$ converge to zero in finite time T which is determined by(18) . This completes the proof. □

Now, the proposed attitude controller is designed using the equivalent control concept. Taking the time derivative of s yields

$$\dot{s} \;=\; \dot{\sigma} + C_1\Lambda_1(\sigma,\alpha)\sigma + C_2\Lambda_2(\sigma,\gamma)\mathrm{sign}(\sigma). \tag{22}$$

Setting $\dot{s} = 0$ and substituting (7) into (22), the equivalent control u_{eq} is obtained as

$$u_{eq} = -B^{-1}\Big(F + C_1\Lambda_1(\sigma,\alpha)\sigma + C_2\Lambda_2(\sigma,\gamma)\mathrm{sign}(\sigma)\Big). \tag{23}$$

Thus, the proposed second order sliding mode attitude controller is designed as

$$u = u_{eq} + u_s, \tag{24}$$

where

$$\begin{aligned} u_s &= -B^{-1}(-\mu_1\Lambda_2(s,\beta)\mathrm{sign}(s) - \mu_2 s + \phi) \\ \dot{\phi} &= -\mu_3\Lambda_2(s,2\beta-1)\mathrm{sign}(s) - \mu_4 s - \mu_5\mathrm{sign}(s), \end{aligned} \tag{25}$$

where $\beta \in (0.5, 1)$ and $\mu_1 = \mathrm{diag}(\mu_{11}, \mu_{12}, \mu_{13})$, $\mu_2 = \mathrm{diag}(\mu_{21}, \mu_{22}, \mu_{23})$, $\mu_3 = \mathrm{diag}(\mu_{31}, \mu_{32}, \mu_{33})$, $\mu_4 = \mathrm{diag}(\mu_{41}, \mu_{42}, \mu_{43})$, $\mu_5 = \mathrm{diag}(\mu_{51}, \mu_{52}, \mu_{53})$ with μ_{1i}, μ_{2i}, μ_{3i}, μ_{4i}, and μ_{5i} $(i = 1, 2, 3)$ being positive constants.

Next, the finite-time stability of the closed-loop system under the proposed SOSMC algorithm is analyzed. This control law can guarantee that the system trajectories converges to the sliding surface $s = 0$ in finite time.

Theorem 3.2. Consider the system (14) and let the Assumptions 2.3 and 2.4 hold. Under the control law (25) with the sliding surface (16) , the sliding variable s and its first time derivative $\dot{s}$ converge to a residual set of zero in finite time.

Proof. Substituting the control law (25) into (22), one obtains the closed-loop system as

$$\dot{s} = -\mu_1\Lambda_2(s,\beta)\mathrm{sign}(s) - \mu_2 s + \phi + \tilde{d} \tag{26}$$

Letting $z_1 = s$ and $z_2 = \phi + \tilde{d}$, the auxiliary variable dynamics can be obtained as can be established in the scalar form $(i = 1, 2, 3)$ as

$$\begin{aligned} \dot{z}_{1i} &= -\mu_{1i}|z_{1i}|^{\beta}\mathrm{sign}(z_{1i}) - \mu_{2i}z_{1i} + z_{2i} \\ \dot{z}_{2i} &= -\mu_{3i}|z_{1i}|^{(2\beta-1)}\mathrm{sign}(z_{1i}) - \mu_{4i}z_{1i} - \mu_{5i}\mathrm{sign}(z_{1i}) + \chi_i, \end{aligned} \tag{27}$$

where $\chi_i = \dot{\tilde{d}}_i$.

Consider the following candidate strict Lyapunov function

$$\begin{aligned} V_2(z) \;=\; & \frac{\mu_{3i}}{\beta}|z_{1i}|^{2\beta} + \mu_{4i}z_{1i}^2 + \frac{1}{2}z_{2i}^2 + 2\mu_{5i}|z_{1i}| \\ & + \frac{1}{2}\left(z_{2i} - \mu_{1i}|z_{1i}|^{\beta}\mathrm{sign}(z_{1i}) - \mu_{2i}z_{1i}\right)^2, \end{aligned} \tag{28}$$

which can be written as

$$V_2(z) = \nu^T \Pi_1 \nu, \tag{29}$$

where $\nu = [|z_{1i}|^\beta \mathrm{sign}(z_{1i}) \quad |z_{1i}|^{\frac{1}{2}} \quad z_{1i} \quad z_{2i}]^T$ and

$$\Pi_1 = \frac{1}{2}\begin{bmatrix} \frac{2\mu_{3i}}{\beta} + \mu_{1i}^2 & 0 & \mu_{1i}\mu_{2i} & -\mu_{1i} \\ 0 & 4\mu_{5i} & 0 & 0 \\ \mu_{1i}\mu_{2i} & 0 & (2\mu_{4i} + \mu_{2i}^2) & -\mu_{2i} \\ -\mu_{1i} & 0 & -\mu_{2i} & 2 \end{bmatrix}.$$

It satisfies

$$\sigma_{\min}(\Pi_1)\|\nu\|^2 \le V_2 \le \sigma_{\max}(\Pi_1)\|\nu\|^2, \tag{30}$$

where $\|\nu\|^2 = |z_{1i}|^{2\beta} + |z_{1i}| + z_{1i}^2 + z_{2i}^2$, and $\sigma_{\min}(\Pi_1)$ and $\sigma_{\max}(\Pi_1)$ are the minimum and maximum singular values of Π_1. Taking time derivative to (28), one obtains

$$\begin{aligned} \dot{V}_2(z) \;=\; & \Big(2\mu_{3i} + \beta\mu_{1i}^2\Big)|z_{1i}|^{2\beta-1}\mathrm{sign}(z_{1i})\dot{z}_{1i} + (2\mu_{4i} + \mu_{1i}^2)z_{1i}\dot{z}_{1i} \\ & + 2z_{2i}\dot{z}_{2i} + \mu_{1i}\mu_{2i}(\beta+1)|z_{1i}|^\beta\mathrm{sign}(z_{1i})\dot{z}_{1i} - \mu_{2i}z_{1i}\dot{z}_{2i} \\ & - \mu_{2i}z_{2i}\dot{z}_{1i} - \mu_{1i}|z_{1i}|^{\beta-1}z_{1i}\dot{z}_{2i} - \beta\mu_{1i}|z_{1i}|^{\beta-1}z_{2i}\dot{z}_{1i} \\ & + 2\mu_{5i}\mathrm{sign}(z_{1i})\dot{z}_{1i}. \end{aligned} \tag{31}$$

Substituting (27) into (31), one has

$$\begin{aligned} \dot{V}_2(z) \;=\; & \Big(2\mu_{3i} + \beta\mu_{1i}^2\Big)|z_{1i}|^{2\beta-1}\mathrm{sign}(z_{1i})\Big(- \mu_{1i}|z_{1i}|^\beta\mathrm{sign}(z_{1i}) - \mu_{2i}z_{1i} \\ & + z_{2i}\Big) + (2\mu_{4i} + \mu_{2i}^2)z_{1i}\Big(- \mu_{1i}|z_{1i}|^\beta\mathrm{sign}(z_{1i}) - \mu_{2i}z_{1i} + z_{2i}\Big) \\ & + 2z_{2i}\Big(- \mu_{3i}|z_{1i}|^{2\beta-1}\mathrm{sign}(z_{1i}) - \mu_{4i}z_{1i} - \mu_{5i}\mathrm{sign}(z_{1i}) + \chi_i\Big) \\ & + \mu_{1i}\mu_{2i}(\beta+1)|z_{1i}|^\beta\mathrm{sign}(z_{1i})\Big(- \mu_{1i}|z_{1i}|^\beta\mathrm{sign}(z_{1i}) - \mu_{2i}z_{1i} + z_{2i}\Big) \\ & - \mu_{2i}z_{1i}\Big(- \mu_{3i}|z_{1i}|^{2\beta-1}\mathrm{sign}(z_{1i}) - \mu_{4i}z_{1i} - \mu_{5i}\mathrm{sign}(z_{1i}) + \chi_i\Big) \\ & - \mu_{2i}z_{2i}\Big(- \mu_{1i}|z_{1i}|^\beta\mathrm{sign}(z_{1i}) - \mu_{2i}z_{1i} + z_{2i}\Big) - \mu_{1i}|z_{1i}|^{\beta-1}z_{1i} \\ & \times\Big(- \mu_{3i}|z_{1i}|^{2\beta-1}\mathrm{sign}(z_{1i}) - \mu_{4i}z_{1i} - \mu_{5i}\mathrm{sign}(z_{1i}) + \chi_i\Big) \\ & - \beta\mu_{1i}|z_{1i}|^{\beta-1}z_{2i}\Big(- \mu_{1i}|z_{1i}|^\beta\mathrm{sign}(z_{1i}) - \mu_{2i}z_{1i} + z_{2i}\Big) \\ & + 2\mu_{5i}\mathrm{sign}(z_{1i})\Big(- \mu_{1i}|z_{1i}|^\beta\mathrm{sign}(z_{1i}) - \mu_{2i}z_{1i} + z_{2i}\Big). \end{aligned} \tag{32}$$

Multiplying out brackets, one obtains

$$\begin{aligned}
\dot{V}_2(z) \; = \; & -\mu_{1i}\Big(2\mu_{3i}+\beta\mu_{1i}^2\Big)|z_{1i}|^{(2\beta-1)}|z_{1i}|^{\beta}-\mu_{2i}\Big(2\mu_{3i} \\
& +\beta\mu_{1i}^2\Big)|z_{1i}|^{2\beta}+\Big(2\mu_{3i}+\beta\mu_{1i}^2\Big)|z_{1i}|^{(2\beta-1)}\mathrm{sign}(z_{1i})z_{2i} \\
& -\mu_{1i}(2\mu_{4i}+\mu_{2i}^2)|z_{1i}|^{\beta}\mathrm{sign}(z_{1i})z_{1i}-\mu_{2i}(2\mu_{4i}+\mu_{2i}^2)z_{1i}^2 \\
& +(2\mu_{4i}+\mu_{2i}^2)z_{1i}z_{2i}-2\mu_{3i}|z_{1i}|^{(2\beta-1)}\mathrm{sign}(z_{1i})z_{2i} \\
& -2\mu_{4i}z_{1i}z_{2i}-2\mu_{5i}\mathrm{sign}(z_{1i})z_{2i}-\mu_{1i}^2\mu_{2i}(\beta+1)|z_{1i}|^{2\beta} \\
& -\mu_{1i}\mu_{2i}^2(\beta+1)|z_{1i}|^{\beta+1}+\mu_{1i}\mu_{2i}|z_{1i}|^{\beta}\mathrm{sign}(z_{1i})z_{2i}(\beta+1) \\
& +\mu_{4i}\mu_{2i}z_{1i}^2+\mu_{2i}\mu_{3i}|z_{1i}|^{2\beta}+\mu_{2i}\mu_{5i}|z_{1i}|+\mu_{1i}\mu_{2i}|z_{1i}|^{\beta}\mathrm{sign}(z_{1i})z_{2i} \\
& -\mu_{2i}^2z_{1i}z_{2i}-\mu_{2i}z_{2i}^2-|z_{1i}|^{\beta-1}\Big(-\mu_{1i}\mu_{4i}z_{1i}^2-\mu_{1i}^2|z_{1i}|^{2\beta} \\
& -\mu_{1i}\mu_{5i}|z_{1i}|\Big)-\beta|z_{1i}|^{\beta-1}\Big(-\mu_{1i}^2|z_{1i}|^{\beta}\mathrm{sign}(z_{1i})z_{2i}-\mu_{1i}\mu_{2i}z_{1i}z_{2i} \\
& +\mu_{1i}z_{2i}^2\Big)-2\mu_{5i}\mathrm{sign}(z_{1i})z_{2i}+2\mu_{1i}\mu_{5i}|z_{1i}|^{\beta}+2\mu_{2i}\mu_{5i}|z_{1i}| \\
& +2\chi_iz_{2i}-\mu_{2i}z_{1i}\chi_i-\chi_i\mu_{1i}|z_{1i}|^{\beta}\mathrm{sign}(z_{1i}). \qquad (33)
\end{aligned}$$

After lengthy algebraic manipulation, the derivative of V_2 can be written as

$$\dot{V}_2=-|z_{1i}|^{\beta-1}\nu^T\Omega_1\nu-\nu^T\Omega_2\nu-\chi\Gamma_1\nu, \qquad (34)$$

where

$$\Omega_1=\mu_{1i}\begin{bmatrix}\mu_{3i}+\mu_{1i}^2\beta & 0 & 0 & -\mu_{1i}\beta \\ 0 & \mu_{5i} & 0 & 0 \\ 0 & 0 & \mu_{4i}+\mu_{2i}^2(\beta+2) & -\mu_{2i}(\beta+1) \\ -\mu_{1i}\beta & 0 & -\mu_{2i}(\beta+1) & \beta\end{bmatrix},$$

$$\Omega_2=\mu_{2i}\begin{bmatrix}\mu_{3i}+\mu_{1i}^2(2\beta+1) & 0 & 0 & 0 \\ 0 & \mu_{5i} & 0 & 0 \\ 0 & 0 & \mu_{4i}+\mu_{2i}^2 & -\mu_{2i} \\ 0 & 0 & -\mu_{2i} & 1\end{bmatrix}$$

and

$$\Gamma_1=\begin{bmatrix}\mu_{1i} & 0 & \mu_{2i} & -2\end{bmatrix}.$$

It should be note that to ensure that Ω_1 is positive definite, the condition

$$\mu_{3i}\mu_{4i}>\Big(\frac{\mu_{3i}}{\beta}+(\beta+1)^2\mu_{1i}^2\Big)\mu_{2i}^2 \qquad (35)$$

is required. Also, with positive values of μ_{1i}, μ_{2i}, μ_{3i}, μ_{4i} and μ_{5i}, it is sufficient to ensure that Ω_2 is positive definite.

Therefore, we have

$$\dot{V}_2\leq-|z_{1i}|^{\beta-1}\sigma_{\min}(\Omega_1)\|\nu\|^2-\sigma_{\min}(\Omega_2)\|\nu\|^2+D_2|\Gamma_1\|\|\nu\|. \qquad (36)$$

Using $|z_{1i}|^{\beta-1}\geq\|\nu\|^{\frac{\beta-1}{\beta}}$, one obtains

$$\dot{V}_2\leq-\sigma_{\min}(\Omega_1)\|\nu\|^{\frac{\beta-1}{\beta}}\|\nu\|^2-\sigma_{\min}(\Omega_2)\|\nu\|^2+D_2\|\Gamma_1\|\|\nu\| \qquad (37)$$

We can change (37) into the following forms

$$\dot{V}_2 \leq -\Big(\sigma_{\min}(\Omega_1)\|\nu\|^{\frac{2\beta-1}{\beta}} - D_2\|\Gamma_1\|\Big)\|\nu\| - \sigma_{\min}(\Omega_2)\|\nu\|^2 \tag{38}$$

$$\dot{V}_2 \leq -\Big(\sigma_{\min}(\Omega_2)\|\nu\| - D_2\|\Gamma_1\|\Big)\|\nu\| - \sigma_{\min}(\Omega_1)\|\nu\|^{\frac{3\beta-1}{\beta}} \tag{39}$$

For (38), if we choose the gains such that $\sigma_{min}(\Omega_1)\|\nu\|^{\frac{2\beta-1}{\beta}} \geq D_2\|\Gamma_1\|$, then (38) can be written as

$$\dot{V}_2 \leq -\frac{\eta_1}{\sqrt{\sigma_{\max}(\Pi_1)}}V_2^{0.5} - \frac{\sigma_{\min}(\Omega_2)}{\sigma_{\max}(\Pi_1)}V_2 \tag{40}$$

where $\eta_1 = \sigma_{\min}(\Omega_1)\|\nu\|^{\frac{2\beta-1}{\beta}} - D_2\|\Gamma_1\|$ is a positive scalar. Thus, the trajectories of closed-loop system are bounded ultimately as

$$\lim_{t\to\infty} \vartheta \in \left(\|\vartheta\| > \left(\frac{D_2\|\Gamma_1\|}{\sigma_{\min}(\Omega_1)}\right)^{\frac{\beta}{2\beta-1}}\right),$$

which is a small neighborhoods of the origin of the closed-loop system. This implies that $\|\nu\|$ will converge to the region

$$\|\nu\| \leq \left(\frac{D_2\|\Gamma_1\|}{\sigma_{\min}(\Omega_1)}\right)^{\frac{\beta}{2\beta-1}} \tag{41}$$

in finite time. Similarly, if we choose the gains such that $\sigma_{\min}(\Omega_2)\|\nu\| > D_2\|\Gamma_1\|$, then (39) can be rewritten as

$$\dot{V}_2 \leq -\sigma_{\min}(\Omega_1)\|\nu\|^{\frac{3\beta-1}{\beta}}V_2^{0.5} - \frac{\eta_2}{\sigma_{\max}(\Pi_1)}V_2 \tag{42}$$

where $\eta_2 = \sigma_{\min}(\Omega_2)\|\nu\| - D_2\|\Gamma_1\|$ is a positive scalar. Similar to the previous case, one can conclude that the error system (27) will converge to the region

$$\|\nu\| \leq \frac{D_2\|\Gamma_1\|}{\sigma_{\min}(\Omega_2)} \tag{43}$$

in finite time.

Meanwhile, the gains guarantee that the system trajectory will finite-time converge to the region

$$\begin{aligned} \|\nu\| &\leq \Delta = \min\{\Delta_1, \Delta_2\}, \\ \Delta_1 &= \frac{D_2\|\Gamma_1\|}{\sigma_{\min}(\Omega_2)} \text{and} \quad \Delta_2 = \left(\frac{D_2\|\Gamma_1\|}{\sigma_{\min}(\Omega_1)}\right)^{\frac{\beta}{2\beta-1}}. \end{aligned} \tag{44}$$

Certainly, the design parameters μ_{1i}, μ_{2i}, μ_{3i}, μ_{4i} and μ_{5i} determine the band of the bounded region. If these parameters are appropriately chosen, then $\sigma_{\min}(\Omega_1)$ is adequately large such that $\dot{V}_2 < 0$ when V_2 is out of the bounded region which contains an equilibrium point. This implies that the sliding manifold $s = z_1$ and its time derivative $s = z_2$ will converge to zero in finite time. These parameters can be selected large enough to ensure the motion very close to the sliding manifold. Therefore, the control law (25) ensures that the sliding motion is achieved in finite-time and sustained thereafter. This completes the proof. □

Remark 3.3. The first time derivative of the Lyapunov function (28) is calculated by ignoring the equilibrium point $(z_{1i}, z_{2i}) = (0, 0)$. In practice, the initial states of z_{1i} and z_{2i} are chosen far from the equilibrium point. Then, $\dot{V}_2 < 0$ ensures that the energy of the system decreases and the states z_{1i} and z_{2i} converge to the equilibrium point. At the equilibrium point, the Lyapunov function is $V_2 = 0$. This implies that $z_{1i} = 0$ and $z_{2i} = 0$ are already achieved, so $\dot{V}_2$ is not required. Thus, the case $z_{1i} = 0$ and $z_{2i} = 0$ is not considered in the stability analysis.

Remark 3.4. Note that the system (27) is different from several non-homogeneous super-twisting algorithms presented in Moreno [21] due to the presence of the term $-\mu_{3i}|z_{1i}|^{2\beta-1}\text{sign}(z_{1i})$. Moreover, the control parameters μ_{1i}, μ_{2i}, μ_{3i}, μ_{4i} and μ_{5i} are chosen independently from each other. This term makes the system more complicated and the proof of finite-time stability for the system is rather complicated. However, in this paper a strict Lyapunov function in the form of state variables with an unknown factional power is suggested and it can be used to prove the finite-time stability of (27).

4. ESO-BASED SOSMC

In this section, a new finite-time sliding mode disturbance observer is established to estimate the disturbance for the attitude tracking of flexible spacecraft. Based on the ESO technique [3], an extended state variable is defined as $X_2 = \tilde{d}$. We obtain

$$\begin{aligned} \dot{X}_1 &= F + Bu + X_2 \\ \dot{X}_2 &= \varphi(t), \end{aligned} \tag{45}$$

where φ is the first time derivative of the total disturbance vector $\tilde{d}(t)$. Now let Z_1 and Z_2 be the outputs of the observer. We define $y_1 = Z_1 - X_1$ and $y_2 = Z_2 - X_2$ as the observer errors.

4.1. ESO design

A novel ESO is designed based on the second order sliding mode concept. The proposed disturbance observer is given by

$$\begin{aligned} \dot{Z}_1 &= Z_2 + F + Bu - \Lambda_2(y_1, \beta)\text{sign}(y_{1i}) \\ \dot{Z}_2 &= -\rho_2\Lambda_2(y_1, 2\beta - 1)\text{sign}(y_{1i}) - \rho_3 y_1 - \rho_4(y_1, \beta)\text{sign}(y_{1i}) \\ &\quad -\rho_5\text{sign}(y_1), \end{aligned} \tag{46}$$

where $\rho_1 = \text{diag}(\rho_{11}, \rho_{12}, \rho_{13})$, $\rho_2 = \text{diag}(\rho_{21}, \rho_{22}, \rho_{23})$, $\rho_3 = \text{diag}(\rho_{31}, \rho_{32}, \rho_{33})$, $\rho_4 = \text{diag}(\rho_{41}, \rho_{42}, \rho_{43})$ and $\rho_5 = \text{diag}(\rho_{51}, \rho_{52}, \rho_{53})$, with ρ_{1i}, ρ_{2i}, ρ_{3i}, ρ_{4i}, ρ_{5i} $(i = 1, 2, 3)$ being positive constants.

Differentiating y_1 and y_2 with respect to time, the observer error dynamics can be established in the scalar form ($i = 1, 2, 3$) as

$$\begin{aligned} \dot{y}_{1i} &= -\rho_{1i}|y_{1i}|^{\beta}\mathrm{sign}(y_{1i}) + y_{2i} \\ \dot{y}_{2i} &= -\rho_{2i}|y_{1i}|^{2\beta-1}\mathrm{sign}(y_{1i}) - \rho_{3i}y_{1i} - \rho_{4i}|y_{1i}|^{\beta}\mathrm{sign}(y_{1i}) \\ &\quad -\rho_{5i}\mathrm{sign}(y_{1i}) + \varphi_i. \end{aligned} \tag{47}$$

Remark 4.1. The system (47) is different from several non-homogeneous super-twisting algorithms presented in Moreno [21] due to the presence of the terms $\rho_{3i}y_{1i}$ and $-\rho_{4i}|y_{1i}|^{\beta}\mathrm{sign}(y_{1i})$. Again, a new strict Lyapunov function in the form of state variables with an unknown factional power can be used to prove the finite-time stability of (47).

Theorem 4.2. Let Assumptions 2.3 and 2.4 hold. Consider the system plant (45) in the presence of the total disturbance vector $\tilde{d}$ with ESO (46). If there exist suitable observer gains ρ_{1i}, ρ_{2i}, ρ_{3i}, ρ_{4i} and ρ_{5i} such that the condition

$$4\rho_{2i}\rho_{3i} > \left(1 + \frac{4\rho_{2i}}{\rho_{1i}^2\beta}\right)\rho_{4i}^2 \tag{48}$$

is satisfied, then the system trajectory will converge to the neighborhood of the origin as

$$\|\vartheta\| \leq \Upsilon = \left(\frac{D_2\|\Gamma_2\|}{\sigma_{\min}(\Omega_3)}\right)^{\frac{\beta}{2\beta-1}}, \tag{49}$$

where $\vartheta = [|y_{1i}|^{\beta}\mathrm{sign}(y_{1i}) \quad |y_{1i}|^{\frac{1}{2}} \quad y_{1i} \quad y_{2i}]^T$ and $\Upsilon > 0$ is a function of the chosen gains ρ_{1i}, ρ_{2i}, μ_{3i}, and ρ_{4i}. The matrices Ω_3 and Γ_2 will be defined later and $\sigma_{\min}(\Omega_3)$ is the minimum singular value of Ω_3.

P r o o f. Consider the following candidate Lyapunov function

$$V_3(y) = \frac{\rho_{2i}}{\beta}|y_{1i}|^{2\beta} + \rho_{3i}y_{1i}^2 + \frac{1}{2}y_{2i}^2 + 2\rho_{5i}|y_{1i}| + \frac{1}{2}\left(\rho_{1i}|y_{1i}|^{\beta}\mathrm{sign}(y_{1i}) - y_{2i}\right)^2, \tag{50}$$

which can be written as

$$V_3(y) = \vartheta^T\Pi_2\vartheta, \tag{51}$$

where

$$\Pi_2 = \frac{1}{2}\begin{bmatrix} \frac{2\rho_{2i}}{\beta} + \rho_{1i}^2 & 0 & 0 & -\rho_{1i} \\ 0 & 4\rho_{5i} & 0 & 0 \\ 0 & 0 & 2\rho_{3i} & 0 \\ -\rho_{1i} & 0 & 0 & 2 \end{bmatrix}.$$

Then

$$\sigma_{\min}(\Pi_2)\|\vartheta\|^2 \leq V_3 \leq \sigma_{\max}(\Pi_2)\|\vartheta\|^2, \tag{52}$$

where $\|\vartheta\|^2 = |y_{1i}|^{2\beta} + |y_{1i}| + y_{1i}^2 + y_{2i}^2$, and $\sigma_{\min}(\Pi_2)$ and $\sigma_{\max}(\Pi_2)$ are the minimum and maximum singular values of Π_2.

Taking the time derivative of (50), one obtains

$$\begin{aligned}\dot{V}_3(y) &= \Big(2\rho_{2i}+\beta\rho_{1i}^2\Big)|y_{1i}|^{2\beta-1}\mathrm{sign}(y_{1i})\dot{y}_{1i}+2\rho_{3i}y_{1i}\dot{y}_{1i}+2y_{2i}\dot{y}_{2i}\\ &\quad -\rho_{1i}|y_{1i}|^{\beta-1}y_{1i}\dot{y}_{2i}+2\rho_{5i}\mathrm{sign}(y_{1i})\dot{y}_{1i}-\beta\rho_{1i}|y_{1i}|^{\beta-1}y_{2i}\dot{y}_{1i}. \qquad (53)\end{aligned}$$

Substituting (47) into (53), one has

$$\begin{aligned}\dot{V}_3(y) &= \Big(2\rho_{2i}+\beta\rho_{1i}^2\Big)|y_{1i}|^{(2\beta-1)}\mathrm{sign}(y_{1i})\Big(-\rho_{1i}|y_{1i}|^{\beta}\mathrm{sign}(y_{1i})+y_{2i}\Big)\\ &\quad +2\rho_{3i}y_{1i}\Big(-\rho_{1i}|y_{1i}|^{\beta}\mathrm{sign}(y_{1i})+y_{2i}\Big)+2y_{2i}\Big(-\rho_{2i}|y_{1i}|^{2\beta-1}\mathrm{sign}(y_{1i})\\ &\quad -\rho_{3i}y_{1i}-\rho_{4i}|y_{1i}|^{\beta}\mathrm{sign}(y_{1i})-\rho_{5i}\mathrm{sign}(y_{1i})+\varphi_i\Big)-\rho_{1i}|y_{1i}|^{\beta-1}y_{1i}\\ &\quad \times\Big(-\rho_{2i}|y_{1i}|^{2\beta-1}\mathrm{sign}(y_{1i})-\rho_{3i}y_{1i}-\rho_{4i}|y_{1i}|^{\beta}\mathrm{sign}(y_{1i})-\rho_{5i}\mathrm{sign}(y_{1i})+\varphi_i\Big)\\ &\quad -\beta\rho_{1i}|y_{1i}|^{\beta-1}\mathrm{sign}(y_{1i})y_{2i}\Big(-\rho_{1i}|y_{1i}|^{\beta}\mathrm{sign}(y_{1i})+y_{2i}\Big)\\ &\quad +\rho_{5i}\mathrm{sign}(y_{1i})\Big(-\rho_{1i}|y_{1i}|^{\beta}\mathrm{sign}(y_{1i})\\ &\quad +y_{2i}\Big)+\rho_{5i}\mathrm{sign}(y_{1i})\Big(-\rho_{1i}|y_{1i}|^{\beta}\mathrm{sign}(y_{1i})+y_{2i}\Big). \qquad (54)\end{aligned}$$

Multiplying out brackets, one has

$$\begin{aligned}\dot{V}_3(y) &= -\rho_{1i}\Big(2\rho_{2i}+\beta\rho_{1i}^2\Big)|y_{1i}|^{(2\beta-1)}|y_{1i}|^{\beta}+\Big(2\rho_{2i}+\beta\rho_{1i}^2\Big)|y_{1i}|^{(2\beta-1)}\mathrm{sign}(y_{1i})y_{2i}\\ &\quad -2\rho_{1i}\rho_{3i}|y_{1i}|^{\beta+1}+2\rho_{3i}y_{1i}y_{2i}-2\rho_{2i}|y_{1i}|^{(2\beta-1)}\mathrm{sign}(y_{1i})y_{2i}-2\rho_{3i}y_{1i}y_{2i}\\ &\quad -2\rho_{4i}|y_{1i}|^{\beta}\mathrm{sign}(y_{1i})y_{2i}-2\rho_{5i}\mathrm{sign}(y_{1i})y_{2i}-|y_{1i}|^{\beta-1}\Big(-\rho_{1i}\rho_{3i}y_{1i}^2-\rho_{1i}\rho_{2i}|y_{1i}|^{2\beta}\\ &\quad -\rho_{1i}\rho_{4i}|y_{1i}|^{\beta+1}\Big)-\beta|y_{1i}|^{\beta-1}\Big(-\rho_{1i}^2|y_{1i}|^{\beta}\times\mathrm{sign}(y_{1i})y_{2i}-\rho_{1i}\rho_{2i}y_{1i}y_{2i}+\rho_{1i}y_{2i}^2\Big)\\ &\quad +2\varphi_i y_{2i}-\varphi_i\rho_{1i}|y_{1i}|^{\beta}\mathrm{sign}(y_{1i})-2\rho_{1i}\rho_{5i}|y_{1i}|+2\rho_{5i}\mathrm{sign}(y_{1i})y_{2i}. \qquad (55)\end{aligned}$$

After some algebraic manipulation, we can obtain

$$\dot{V}_3=-|y_{1i}|^{\beta-1}\vartheta^T\Omega_3\vartheta-\varphi\Gamma_2\vartheta, \qquad (56)$$

where

$$\Omega_3=\rho_{1i}\begin{bmatrix}\rho_{2i}+\rho_{1i}^2\beta & 0 & -\dfrac{\rho_{4i}}{2} & -\rho_{1i}\beta\\ 0 & \rho_{5i} & 0 & 0\\ -\dfrac{\rho_{4i}}{2} & 0 & \rho_{3i} & \dfrac{\rho_{4i}}{\rho_{1i}}\\ -\rho_{1i}\beta & 0 & \dfrac{\rho_{4i}}{\rho_{1i}} & \beta\end{bmatrix},$$

and

$$\Gamma_2=\begin{bmatrix}\rho_{1i} & 0 & 0 & -2\end{bmatrix}.$$

It should be noted that the condition (48) is required to guarantee that Ω_3 is positive definite.

From (56), we obtain

$$\dot{V}_3 \leq -|y_{1i}|^{\beta-1}\sigma_{\min}(\Omega_3)\|\vartheta\|^2 + D_2\|\Gamma_2\|\|\vartheta\|. \tag{57}$$

Using $|y_{1i}|^{\beta-1} \geq \|\vartheta\|^{\frac{\beta-1}{\beta}}$, one obtains

$$\dot{V}_3 \leq -\sigma_{\min}(\Omega_3)\|\vartheta\|^{\frac{\beta-1}{\beta}}\|\vartheta\|^2 + D_2\|\Gamma_2\|\|\vartheta\|. \tag{58}$$

We can now change (58) into the following form

$$\dot{V}_3 \leq -\Big(\sigma_{\min}(\Omega_3)\|\vartheta\|^{\frac{2\beta-1}{\beta}} - D_2\|\Gamma_2\|\Big)\|\vartheta\|. \tag{59}$$

From (52) we know that $\|\vartheta\|^2 \geq \dfrac{V_3}{\sigma_{\max}(\Pi_2)}$. Next, if we choose the gains such that $\sigma_{\min}(\Omega_3)\|\vartheta\|^{\frac{2\beta-1}{\beta}} \geq D_2\|\Gamma_2\|$, then (59) can be written as

$$\dot{V}_3 \leq -\frac{\eta_1}{\sqrt{\sigma_{\max}(\Pi_2)}}V_3^{1/2}, \tag{60}$$

where $\eta_1 = \sigma_{\min}(\Omega_3)\|\vartheta\|^{\frac{2\beta-1}{\beta}} - D_2\|\Gamma_2\|$ is a positive scalar. The decrease of V_3 finally forces the trajectories of the closed-loop system into $\|\vartheta\| > \left(\dfrac{D_2\|\Gamma_2\|}{\sigma_{\min}(\Omega_3)}\right)^{\frac{\beta}{2\beta-1}}$. Thus, the trajectories of closed-loop system are bounded ultimately as

$$\lim_{t\to\infty} \vartheta \in \left(\|\vartheta\| > \left(\frac{D_2\|\Gamma_2\|}{\sigma_{\min}(\Omega_3)}\right)^{\frac{\beta}{2\beta-1}}\right), \tag{61}$$

which is a small set containing the origin of the closed-loop system. This implies that $\|\vartheta\|$ will approach to the region

$$\|\vartheta\| \leq \Upsilon = \left(\frac{D_2\|\Gamma_2\|}{\sigma_{\min}(\Omega_3)}\right)^{\frac{\beta}{2\beta-1}}. \tag{62}$$

is reached in finite time. □

Remark 4.3. If the gains ρ_{1i}, ρ_{2i}, ρ_{3i}, ρ_{4i} and ρ_{5i} are selected such that the condition (48) is satisfied, then by Lemma 2.1 the finite-time convergence property can be obtained. These gains will also guarantee that the system trajectory will converge to the region (49) in finite time. In fact, we can choose ρ_{1i}, ρ_{2i}, ρ_{3i} and ρ_{4i} such that $\frac{D_2\|\Gamma_2\|}{\sigma_{\min}(\Omega_3)} < 1$. With $\beta \in (0.5, 1)$, $\frac{\beta}{2\beta-1}$ is sufficiently large, so Υ can be greatly reduced. This means that the proposed control has strict robustness and disturbance rejection ability.

Remark 4.4. For the system (47), when $\beta = \frac{1}{2}$, $\rho_{2i} = \rho_{3i} = \rho_{4i} = 0$, the structure (47) becomes the form of the observer by Davila et al. [15]. Thus, the proposed observer is the generalized version of the observer by Davila et al. [15]. The proposed method gives an additional appealing feature that it offers more choices to tune this observer to achieve an improved performance. Since the observer (46) has a complicated form, the stability analysis of observer error dynamics is rather difficult and has not been proposed. In this paper, this observer is used to estimate unknown disturbances, while the observer by Davila et al. [15] is applied estimate unknown system states.

4.2. Controller design

The anti-disturbance feedback attitude tracking controller can be designed using the observer outputs Z_1 and Z_2 in (46) instead of the actual error derivatives X_1 and X_2. Also, the proposed extended state observer-based second order sliding mode control (ESO-based SOSMC) law is defined as

$$u = u_{eq} + u_s - B^{-1} Z_2. \tag{63}$$

Remark 4.5. By combining the sliding mode disturbance observer to estimate the total disturbance $\tilde{d}$, the developed controller (63) achieves disturbance rejection. It can be seen from the above that the realization of this controller does not require accurate dynamic model because the the proposed ESO does not need explicit knowledge of the function $\varphi(t)$.

Remark 4.6. Similar to our proposed control method, the traditional PID controller can force the states of the closed-loop system to converge to a small region of the origin in finite time. However, it cannot ensure the robustness against the uncertainties and disturbances. Moreover, based on the concepts of SOSMC, our proposed control method usually yields higher accuracy than the traditional PID controller. Although, the sliding surface is designed by adapting the terminal sliding mode concepts, the controller is not directly developed by fast terminal sliding mode reaching law [30]. The generalized super twisting control algorithm is employed to developed the controller. This controller can achieve the better performance than the terminal sliding mode controller and super twisting algorithm. Unlike the quasi-continuous controller, the proposed controller does not require the first time derivative of the sliding variable. This makes it easier to implement. Moreover, the disturbance observer is also developed to compensate for disturbances. This helps the proposed method can effectively achieve high accuracy and fast convergence rate.

5. SIMULATIONS

Numerical simulations on the flexible spacecraft have been conducted to verify the performance of the proposed ESO-based SOSMC (63) and the robust finite-time control (RFTC) method in [30]. The same model parameters used in [6] are applied in this study. The inertia matrix and the flexible coupling matrix are as follows

$$J = \begin{bmatrix} 350 & 3 & 4 \\ 3 & 270 & 10 \\ 4 & 10 & 190 \end{bmatrix} \quad \mathrm{kg} \cdot \mathrm{m}^2$$

and

$$\delta = \begin{bmatrix} 6.45637 & 1.27814 & 2.15629 \\ -1.25619 & 0.91756 & -1.67264 \\ 1.11678 & 2.48901 & -0.83674 \\ 1.23637 & -2.6581 & -1.12503 \end{bmatrix} \quad \mathrm{kg}^{1/2} \cdot \mathrm{m/s}^2,$$

respectively. The natural frequencies and damping are provided by

$$\begin{aligned} \omega_{n1} &= 0.7681, \quad \omega_{n2} = 1.1038, \quad \omega_{n3} = 1.8733, \quad \omega_{n4} = 2.5496 \quad \text{rad/sec} \\ \xi_1 &= 0.0056, \quad \xi_2 = 0.0086, \quad \xi_3 = 0.013, \quad \xi_1 = 0.025. \end{aligned} \tag{64}$$

In this numerical simulation, we assume that the desired angular velocity is given by

$$\omega_d(t) = 0.05 \begin{bmatrix} \sin(\frac{\pi t}{100}) \\ \sin(\frac{2\pi t}{100}) \\ \sin(\frac{3\pi t}{100}) \end{bmatrix} \quad \text{rad/s.} \tag{65}$$

For the initial conditions of the unit quaternion and the target unit quaternion, we set $Q(0) = [0.3320 \quad -0.4618 \quad 0.1915 \quad 0.7999]^T$ and $Q_d(0) = [0 \quad 0 \quad 0 \quad 1]^T$, respectively. The initial value of the angular velocity is assumed to be $\omega(0) = [0 \quad 0 \quad 0]^T$ rad/s. We bounded the magnitude of the control torque as $|u_i| \leq 4.0$ N-m, $i = 1, 2, 3$. The external disturbance torque that includes constant disturbance and periodic disturbance of two different frequencies is described as follows:

$$d = \begin{bmatrix} 3\cos(t) - 10 + \sin(0.3t) \\ 3\cos(0.5t) + 15 - 1.5\sin(0.2t) \\ 3\sin(t) + 10 + 8\sin(0.4t) \end{bmatrix} \times 10^{-3} Nm.$$

For the RFTC method in [30], simulations are performed with the parameters given as $a = 3$, $b = 5$, $\lambda = 0.2$, $\beta = 0.2$ and $k = 3.5I_3$, where I_3 is the 3×3 identity matrix. For the sliding surface (16), the chosen parameters are given as $C_1 = I_3$, $C_2 = I_3$, $\gamma = \frac{7}{9}$, $\alpha_i = 1.5 \quad (i = 1, 2, 3)$.

The control parameters for the controller (63) are selected to be $\beta = \frac{5}{7}$, $\mu_1 = 2.5I_3$, $\mu_2 = I_3$, $\mu_3 = 5I_3$, $\mu_4 = 7I_3$ and $\mu_5 = 0.5I_3$. For the proposed observer (46), the parameters are given as $\rho_1 = 4.5I_3$, $\rho_2 = 2.5I_3$, $\rho_3 = 1.5I_3$, $\rho_4 = I_3$ and $\rho_5 = 0.3I_3$.

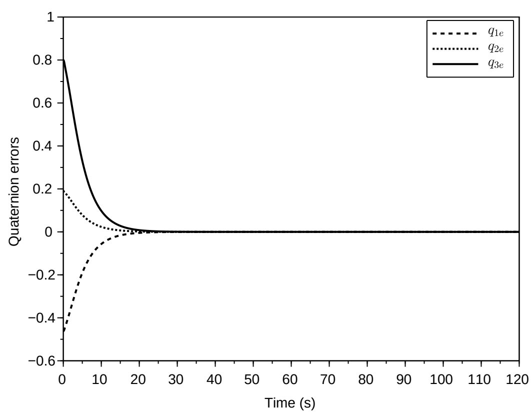

Fig. 1. Responses of quaternion errors under ESO-based SOSMC.

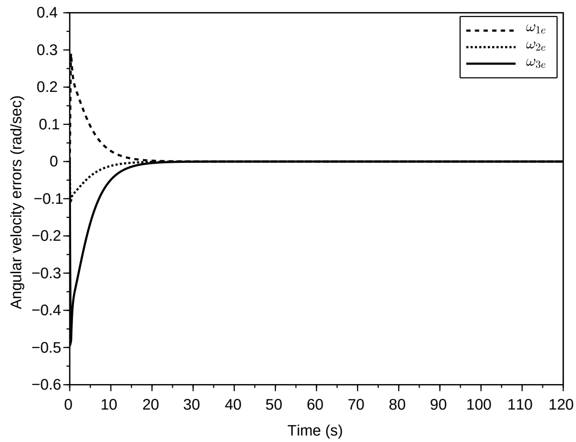

Fig. 2. Responses of angular velocity errors under ESO-based SOSMC.

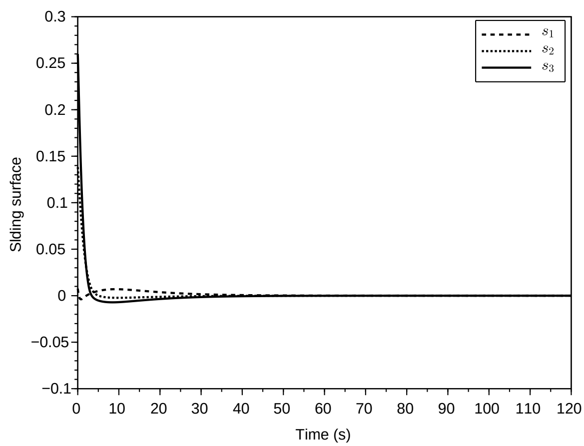

Fig. 3. Responses of sliding variables under ESO-based SOSMC.

As can be seen from Figures 1 and 7, responses of the unit quaternion produced by the controller (63) faster converge to zero than the RFTC method in [30]. As shown in Figures 2 and 8, trajectories of angular velocities generated by the controller (63) are smoother and faster stabilized to zero. Figures 3 and 9 shows responses of sliding variables generated by the controller (63) and RFTC, respectively. The proposed controller (63) exhibits a much quicker convergence of the sliding variables than the RFTC method in [30]. As shown in Figures 4 and 10, control torques produced by the controller (63) are much smoother and faster converge to the steady state level.

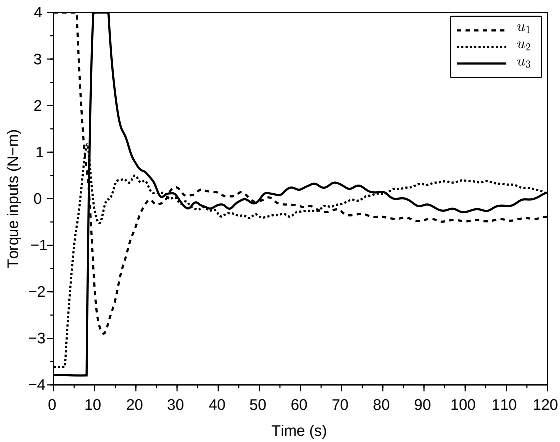

Fig. 4. Profile of control torques under ESO-based SOSMC.

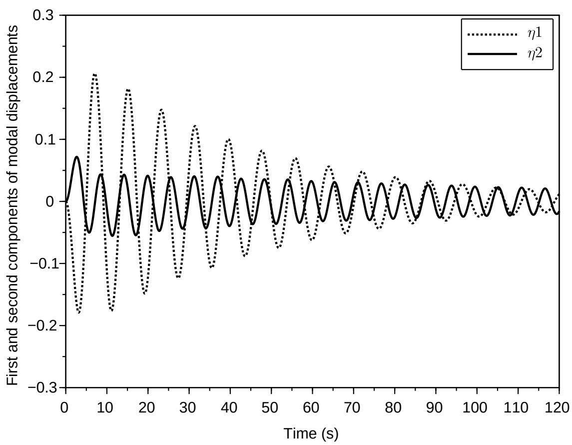

Fig. 5. Responses of flexible modes under ESO-based SOSMC.

Figures 5, 6, 11 and 12 show that for the controller (63), modal coordinates take less time to reach the small neighbourhood of stable. For the RFTC method in [30], tracking accuracies can be listed as follows. During the steady phase, the boundary layer $\|s\| \leq 1\times10^{-4}$ is achieved. The bounds on the final steady state errors are $\|q_e\| \leq 5.6\times10^{-5}$ and $\|\omega_e\| \leq 1.02\times10^{-4}$ with sampling time $h = 0.005$. On the other hand, the controller (63) provides higher tracking accuracy. The boundary layer $\|s\| \leq 3.57 \times 10^{-5}$ is achieved. The bounds on the final steady state errors are $\|q_e\| \leq 1.65\times10^{-5}$ and $\|\omega_e\| \leq 3.16\times10^{-5}$ with sampling time $h = 0.005$. As shown in Figures 13 to 15, the components of the

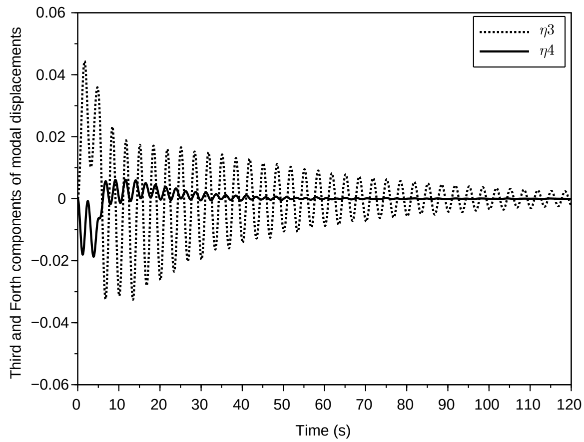

Fig. 6. Responses of flexible modes under ESO-based SOSMC.

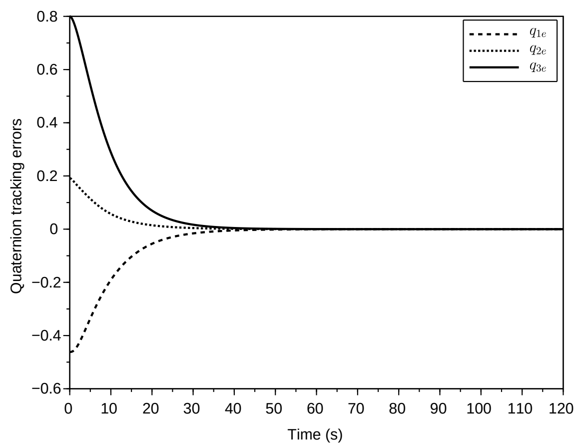

Fig. 7. Responses of quaternion errors under RFTC method.

total disturbance vector are estimated and the observer errors converge to zero within 20 seconds.

Comparing the simulation results obtained from the controller (63) with the RFTC method in [30], we have found the following. The controller (63) offers faster convergence of quaternion and angular velocity tracking errors. Moreover, higher accuracies of tracking results are obtained. Since the sliding surface $s(t) = 0$ is faster achieved, the system more rapidly becomes robust against external disturbances with improved performance.

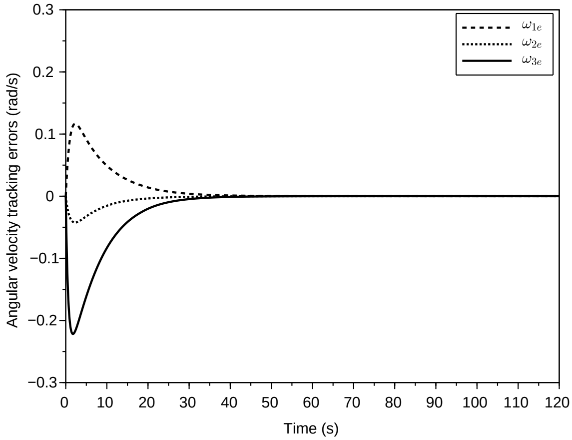

Fig. 8. Responses of angular velocity errors under RFTC method.

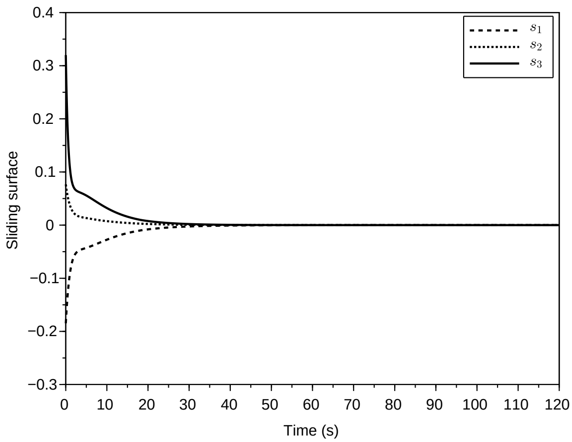

Fig. 9. Responses of sliding variables under RFTC method.

6. CONCLUSION

In this paper, the attitude tracking control problem of a flexible spacecraft is investigated. In the presence of environmental disturbances and inertia uncertainties, the developed attitude control strategy achieves the control objective. Using Lyapunov stability theory, it is proved that the error dynamics converge to a neighborhood of the origin in finite time. The Lyapunov stability theory has been used to ensure the finite time convergence of estimation errors to the desired region containing the origin. By

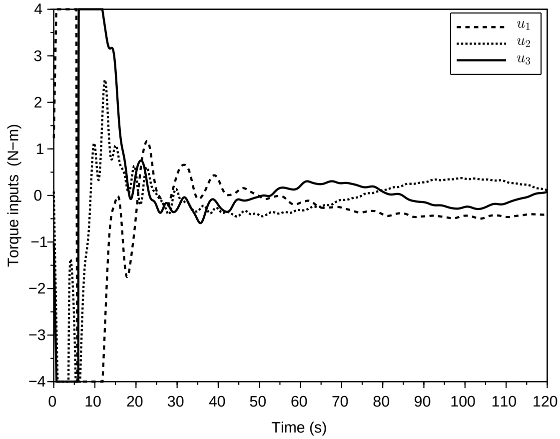

Fig. 10. Profile of control torques under RFTC method

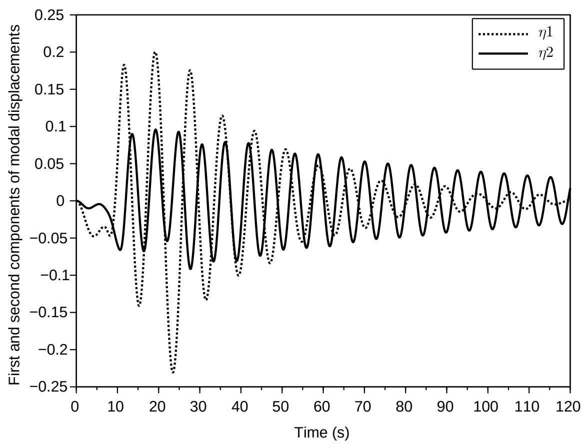

Fig. 11. Responses of flexible modes under RFTC method.

using the proposed ESO, the total disturbance consisting of environmental disturbances, the system uncertainties and flexible vibrations is estimated. Then, with the estimated results, we have derived a new ESO-based SOSMC attitude controller. Numerical simulations on attitude control of a spacecraft model are also provided to demonstrate the performance of the proposed controller.

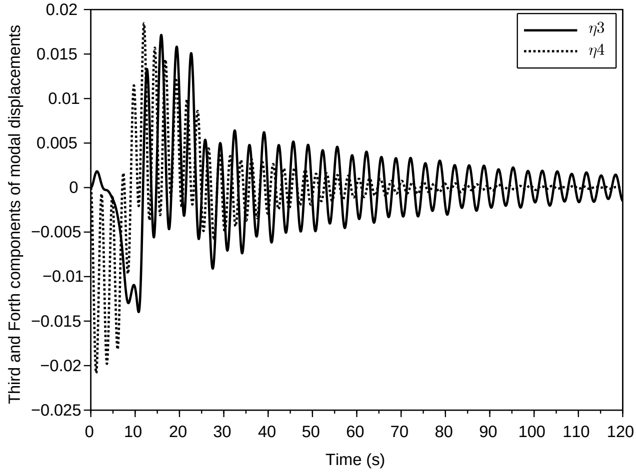

Fig. 12. Responses of flexible modes under RFTC method.

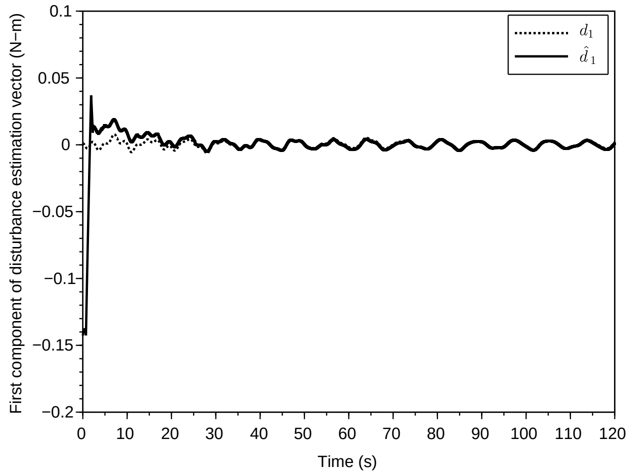

Fig. 13. Estimated angular velocity errors under novel ESO.

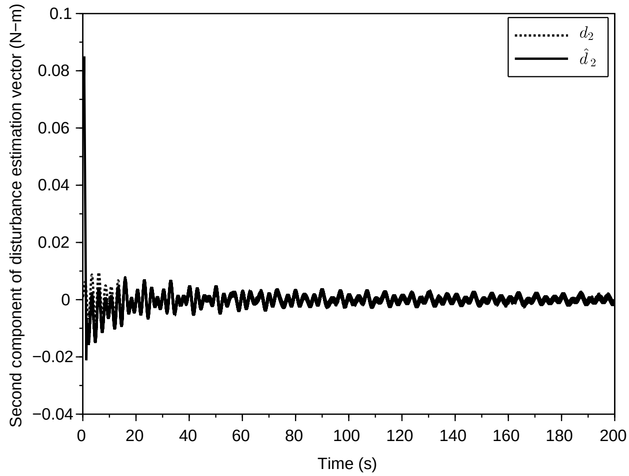

Fig. 14. Estimated angular velocity errors under novel ESO.

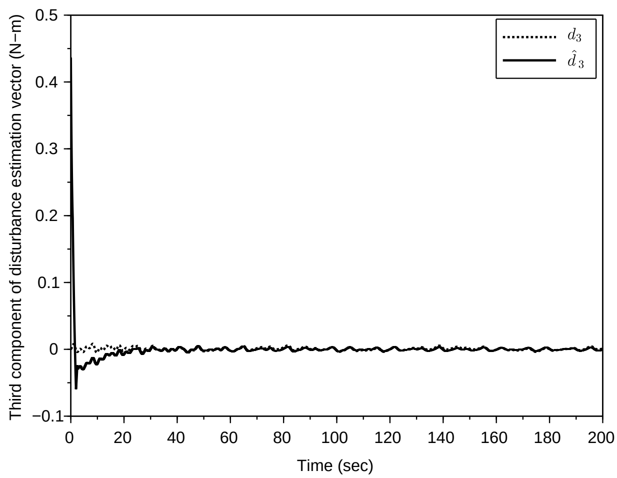

Fig. 15. Estimated angular velocity errors under novel ESO.

ACKNOWLEDGEMENT

The research was funded by King Mongkut's University of Technology North Bangkok. Contract no. KMUTNB-60-ART-50.

(Received December 30, 2016)

REFERENCES

[1] H. Bang, C.-K. Ha, and J. H. Kim: Flexible spacecraft attitude maneuver by application of sliding mode control. Acta Astronautica *57* (2005), 841–850. DOI:10.1016/j.actaastro.2005.04.009

[2] S. Bhat and D. Bernstein: Finite-time stability and continuous autonomus systems. SIAM J. Control. Optim. *38* (2000), 751–766. DOI:10.1137/s0363012997321358

[3] Z. Chen and J. Huang: Attitude tracking and disturbance rejection of rigid spacecraft by adaptive control. IEEE Trans. Automat. Control *54* (2009), 600–605. DOI:10.1109/tac.2008.2008350

[4] Z. Chen and J. Huang: Attitude tracking of rigid spacecraft subject to disturbances of unknown frequencies. Int. J. Robust Nonlinear Control *16* (2014), 2231–2242. DOI:10.1002/rnc.2983

[5] J. Davila, L. Fridman, and A. Levant: Second-order sliding-modes observer for mechanical system. IEEE Trans. Automat. Control *50* (2005), 1785–1789. DOI:10.1109/tac.2005.858636

[6] S. Di Gennaro: Passive attitude control of flexible spacecraft from quaternion measurements. J. Optim. Theory Appl. *116* (2003), 41–60. DOI:10.1023/a:1022106118182

[7] S. Ding and W. X. Zheng: Nonsmooth attitude stabilization of a flexible spacecraft. IEEE Trans. Aerosp. Electron. Syst *50* (2014), 1163–1181. DOI:10.1109/taes.2014.120779

[8] H. Du, S. Li, and C. Qian: Finite-time attitude tracking control of spacecraft with application to attitude synchronization. IEEE Trans. Automat. Control *56* (2011), 2711–2717. DOI:10.1109/tac.2011.2159419

[9] J. Erdong and S. Zhaowei: Passivity-based control for a flexible spacecraft in the presence of disturbances. Int. J. Non-Linear Mech. *45* (2010), 348–356. DOI:10.1016/j.ijnonlinmec.2009.12.008

[10] Y. Feng, X. Yu, and Z. Man: Non-singular terminal sliding mode control of rigid manipulators. Automatica *38* (2002), 2159–2167. DOI:10.1016/s0005-1098(02)00147-4

[11] Q. Hu: Robust adaptive sliding mode attitude control and vibration damping of flexible spacecraft subject to unknown disturbance and uncertainty. Trans. Inst. Measurement and Control *34* (2012), 436–447. DOI:10.1177/0142331210394033

[12] Q. Hu, B. Jiang, and M. Friswell: Robust saturated finite time output feedback attitude stabilization for rigid spacecraft. J. Guid. Control Dyn. *37* (2014), 1914–1929. DOI:10.2514/1.g000153

[13] Q. Hu, Z. Wang, and H. Gao: Sliding mode and shaped input vibration control of flexible systems. IEEE Trans. Aerosp. Electron. Syst. *44* (2008), 503–519. DOI:10.1109/taes.2008.4560203

[14] Y. Jiang, Q. Hu, and G. Ma: Adaptive backstepping fault-tolerant control for flexible spacecraft with unknown bounded disturbances and actuator failures. ISA Trans. *49* (2010), 57–69. DOI:10.1016/j.isatra.2009.08.003

[15] A. Levant: Sliding order and sliding accuracy in sliding mode control. Int. J. Control *58* (1993), 1247–1263. DOI:10.1080/00207179308923053

[16] B. Li, Q. Hu, and G. Ma: ‘Extended state observer based robust attitude control of spacecraft with input saturation. Aerosp. Sci. Technol. *40* (2016), 173–182. DOI:10.1016/j.ast.2015.12.031

[17] J. Li, Y. Pan, and K. D. Kumar: Design of asymptotic second-order sliding mode control for satellite formation flying. J. Guid. Control Dyn. *35* (2015), 309–316. DOI:10.2514/1.55747

[18] S. H. Li, Z. Wang, and S. M. Fei: ‘Comments on the paper: Robust controllers design with finite time convergence for rigid spacecraft attitude tracking. Aerosp. Sci. Technol. *15* (2011), 193–195. DOI:10.1016/j.ast.2010.11.005

[19] W. Luo, Y. C. Chung, and K. V. Ling: Inverse optimal adaptive control for attitude tracking spacecraft. IEEE Trans. Automat. Control *50* (2005), 1639–1654. DOI:10.1109/tac.2005.858694

[20] Z. H. Man, A. P. Paplinski, and H. R. Wu: A robust MIMO terminal sliding mode control scheme for rigid robotic manipulators. IEEE Trans. Automat. Control *39* (1994), 2464–2469. DOI:10.1109/9.362847

[21] J. A. Moreno: On strict Lyapunov functions for some non-homogeneous super-twisting algorithms. J. Franklin Inst. *351* (2014), 1902–1919. DOI:10.1016/j.jfranklin.2013.09.019

[22] E. Moulay and W. Perruquetti: Finite-time stability and continuous autonomous systems. J. Math. Anal. Appl. *323* (2006), 1430–1443. DOI:10.1016/j.jmaa.2005.11.046

[23] C. Pukdeboon and P. Kumam: Robust optimal sliding mode control for spacecraft position and attitude maneuvers. Aerosp. Sci. Technol. *43* (2015), 329–342. DOI:10.1016/j.jmaa.2005.11.046

[24] C. Pukdeboon and P. Siricharuanun: Nonsingular terminal sliding mode based finite-time control for spacecraft attitude tracking. Int. J. Control Automat. Syst. *12* (2014), 530–540. DOI:10.1007/s12555-013-0247-x

[25] C. Pukdeboon, A. S. I. Zinober, and M.-W. L. Thein: Quasi-continuous higher-order sliding mode controllers for spacecraft attitude tracking manoeuvres. IEEE Trans. Ind. Electron. *57* (2010), 1436–1444. DOI:10.1109/tie.2009.2030215

[26] Y. B. Shtessel, I. A Shkolnikov, and A. Levant: A. Smooth second-order sliding modes: Missile guidance application. Automatica *43* (2007), 1470–1476. DOI:10.1016/j.automatica.2007.01.008

[27] Z. Song, H. Li, and K. Sun: Finite-time control for nonlinear spacecraft attitude based on terminal sliding mode technique. ISA Trans. *53* (2014), 117–124. DOI:10.1016/j.isatra.2013.08.008

[28] P. M. Tiwari, S. Janardhanan, and M. un Nabi: Rigid spacecraft attitude control using adaptive integral second order sliding mode. Aerosp. Sci. Technol. *42* (2015), 50–57. DOI:10.1016/j.ast.2014.11.017

[29] V. Utkin: Sliding Modes in Control and Optimization. Springer-Verlag, Berlin 1992.

[30] S. Wu, G. Radice, and Z. Sun: Robust finite-time control for flexible spacecraft attitude maneuver. J. Aerosp. Engrg. *27* (2014), 185–190. DOI:10.1061/(asce)as.1943-5525.0000247

[31] Y. Wu, X. Yu, and Z. Man: Terminal sliding mode control design for uncertain dynamic system. Syst. Control Lett. *34* (1998), 281–288. DOI:10.1016/s0167-6911(98)00036-x

[32] Y. Xia, Z. Zhu, M. Fu, and S. Wang: Attitude tracking of rigid spacecraft with bounded disturbances. IEEE Trans. Ind. Electron. *58* (2011), 647–659. DOI:10.1109/tie.2010.2046611

[33] S. Yu, X. Yu, B. Shirinzadeh, and Z. Man: Continuous finite-time control for roboti manipulators with terminal sliding mode. Automatica *41* (2005), 1957–1964. DOI:10.1109/tie.2010.2046611

[34] D. Zhao, S. Li, and F. Gao: A new terminal sliding mode control for robotic manipulators. Int. J. Control *82* (2009), 1804–1813. DOI:10.1080/00207170902769928

[35] C. X. Zhong, Y. Guo, Z. Yu, L. Wang, and Q. W. Chen: Finite-time attitude control for flexible spacecraft with unknown bounded disturbance. Trans. Institute of Measurement and Control *38* (2016), 2, 240–249. DOI:10.1177/0142331214566223

Chutiphon Pukdeboon, Nonlinear Dynamic Analysis Research Center, Department of Mathematics, Faculty of Applied Science, King Mongkut's University of Technology North Bangkok, Bangkok 10800. Thailand.
e-mail: chutiphon.p@sci.kmutnb.ac.th

Anuchit Jitpattanakul, Department of Mathematics, Faculty of Applied Science, King Mongkut's University of Technology North Bangkok, Bangkok 10800. Thailand.
e-mail: anuchit.j@sci.kmutnb.ac.th